ELSEVIER

Advances in Colloid and Interface Science
70 (1997) 171–210

ADVANCES IN COLLOID AND INTERFACE SCIENCE

Analysis of small-angle scattering data from colloids and polymer solutions: modeling and least-squares fitting[1]

Jan Skov Pedersen

Department of Solid State Physics, Risø National Laboratory, DK-4000 Roskilde, Denmark

Abstract

Analysis and modeling of small-angle scattering data from systems consisting of colloidal particles or polymers in solution are discussed. The analysis requires application of least-squares methods, and the basic principles of linear and non-linear least-squares methods are summarized with emphasis on applications in the analysis of small-angle scattering data. These include indirect Fourier transformation, square-root deconvolution, size distribution determinations, and modeling. The inclusion of corrections for instrumental smearing effects is also discussed. The most common analytical expressions for model form factors and structure factors are summarized. An example of analysis of small-angle neutron and X-ray scattering data from block copolymer micelles is given.

1. Introduction

The article concerns analysis of small-angle scattering data from colloidal and polymer systems consisting of particles or molecules in a solvent. Only systems with short range order and isotropic scattering spectra, for which the scattering intensity is only a function of the

[1] A previous version of this review was used as lecture notes in The Third European Summer School on "Scattering Methods Applied to Soft Condensed Matter", Bombannes, France, 1996.

0001-8686/97/$32.00
PII: S0001-8686(97)00312-0

modulus of the scattering vector are considered. Both X-ray and neutron scattering are treated, however, the more detailed discussion of the program implementations, in particular those concerning instrumental smearing, have emphasis on neutron scattering. It is the intention that the notes can serve as a practical guide in analyzing small-angle scattering data. They contain a relatively brief, but self-contained, description of linear and non-linear least-squares methods with emphasis on the applications in the analysis of small-angle scattering data. The notes also contain a large collection of form factor and structure factors, which are convenient to have at hand when analyzing experimental data.

Small-angle scattering data are usually analyzed either by *model-independent* approaches or by *direct modeling*. Both of these approaches require the application of least-squares methods. The model-independent approaches may consist of a Fourier transformation of the experimental scattering curve, which provides the pair distance distribution function $p(r)$ or, equivalently, the correlation function $\gamma(r)$, where the relation is: $p(r) = r^2\gamma(r)$. The Fourier transformation is usually done by the Indirect Fourier Transformation (IFT) method introduced by Glatter [1,2]. This method can be applied for all systems for which the correlations have a finite range. It has several advantages compared to a direct Fourier transformation, as it allows corrections for instrumental smearing effects and it does not require extrapolations of the data. The $p(r)$ function provides real-space information and comparisons to model calculation may provide key information and give suggestions for the structure of the particles [2,3]. After interpretation of the $p(r)$ function it may be possible to construct a model on an analytical form, which can be fitted to the data. For particles with centro symmetry it is possible to go one step further with the model-independent analysis and perform a SQuare-root DEConvolution (SQDEC) of $p(r)$ as described by Glatter, so that the radial scattering length density profile $\rho(r)$ is obtained [4,5]. The information obtained by this procedure would of course also be incorporated in later attempts to perform model fits to the data. The indirect Fourier transformation requires the application of a *linear least-squares method*, whereas the square-root deconvolution procedure requires the application of *non-linear least-squares methods*.

For polydisperse systems, the aim of the analysis is to extract the size distribution of the particles when a particular shape of the particles is assumed. For very dilute systems, this can be done with a free-form size distribution [6] by a linear least-squares method, which may include a

non-negativity constraint [7]. For systems with a finite concentration of particles which interact with a hard-sphere potential, the size distribution can also be determined on a free-form, but this requires a non-linear least-squares method [7].

For systems with a collection of monodisperse particles, there exists a method for determining the shape of particles model independently by fitting directly to the scattering data. This requires that the particles have a nearly homogeneous distribution of scattering length density. A multipole expansion is used for the shape of the particles and the coefficients of this expansion are determined by non-linear least-squares methods [8,9]. The method has been modified so that it can be used for shape determination of the components of 'two-phase' particles [9], and it has been applied successfully to the 50S subunit of the ribosome of *E. coli* [10–12].

When applying the least-squares methods, it is important that the scientist understand the basic principles, so that the computer programs do not entirely work as a "black box". With some basic understanding it is possible to avoid the most common pitfalls and to understand, why the program 'reacts' as it does, and perhaps, if the applied procedure fails, to choose another strategy which works better. Section 2 of the present notes gives an overview of the least-squares methods. Some of the most common available small-angle scattering model expressions are summarized in Section 3, whereas an example of modeling of small-angle scattering data from block copolymer micelles is given in Section 3.

2. Least-squares Methods

There exist many excellent books on least-squares methods. Two of these are the book by Bevington [13] "Data Reduction and Error Analysis for the Physical Sciences" and the book by Press, Flannery, Teukolsky, and Vetterling [14] "Numerical Recipes". The book by Bevington gives a good introduction as well as a description of the most common methods without excessive use of mathematics. The book by Press, Flannery, Teukolsky, and Vetterling describes in addition some of the numerical aspects and problems when implementing the method. It should also be noted that this book is very useful when implementing complex model expressions as it contains a large collection of routines for special functions.

The least-squares method employs the chi-squared (χ^2)function as a measure for the deviation between the experimental data and the model. Let $I^{exp}(q_i)$, $i = 1,...,N$ be the data points measured for the independent variable q_i. In a scattering experiment $I^{exp}(q_i)$ is the measured intensities and q_i is the modulus of the scattering vector. The counting statistics will give rise to the statistical uncertainties σ_i on the data point $I^{exp}(q_i)$. The *chi-squared* is defined as:

$$\chi^2 \equiv \sum_{i=1}^{N} \left(\frac{I^{exp}(q_i) - (I^{mod}(q_i)}{\sigma_i} \right)^2 \tag{1}$$

where $I^{mod}(q_i)$ is the model intensities which depends on the parameters a_i, $i = 1,...,M$. It is often convenient to consider the *reduced chi-squared* χ_r^2, which is given by:

$$\chi_r^2 = \frac{\chi^2}{N - M} \tag{2}$$

where N–M is the *number of degrees of freedom*. The optimum set of parameter values for a model is determined by minimizing Eq. (1). A fit with $\chi_r^2 = 1$ is considered to be an ideal fit. Note that for $N >> M$ a fit with $\chi_r^2 = 1$ has 'on average' $|I^{exp}(q_i) - I^{mod}(q_i)| = \sigma_i$, which means that the deviations are on average equal to the statistical uncertainties. A more rigorous discussion of the chi-squared function can be found in the text books mentioned above.

2.1 Linear Method

The model intensity function is linear, if it can be written as:

$$I^{mod}(q) = \sum_{k=1}^{M} a_k X_k(q) \tag{3}$$

where $X_k(q)$ is a set of basis functions. This is the case for the indirect Fourier transformation [1,2] for which the distance distribution function is written as:

$$p(r) = \sum_{k=1}^{M} a_k B_k(r) \tag{4}$$

where $B_k(r)$ are cubic b splines. These are bell-shaped functions, composed of piecewise third-order polynomials. One has

$$I^{\text{mod}}(q) = 4\pi \int p(r) \frac{\sin(qr)}{qr} dr = \sum_{k=1}^{M} a_k X_k(q) \tag{5}$$

where

$$X_k(q) = 4\pi \int B_k(r) \frac{\sin(qr)}{qr} dr \tag{6}$$

Alternative linear approaches for performing the IFT have been described by Moore [15], Svergun, Semenyuk and Feigin [16] and Svergun [17]. Note that the maximum entropy method, which also can be used, does give rise to a linear problem [18].

The determination of size distributions on a free form is also a linear problem. In this case

$$I^{\text{mod}}(q) = \Delta\rho^2 \int N(R) F^2(q,R) dR \tag{7}$$

where $\Delta\rho$ is the scattering length density contrast, $N(r)$ is the size distribution and $F(q,r)$ is the form factor amplitude. For homogeneous spheres:

$$F(q,R) = \frac{4\pi}{3} R^3 \frac{3[\sin(qR) - qR\cos(qR)]}{(qR)^3} \tag{8}$$

Setting:

$$N(R) = \sum_{k=1}^{M} a_k B_k(R) \tag{9}$$

where $B_k(R)$ are cubic [6] or linear [7] b splines, the model intensity becomes

$$I^{\mathrm{mod}}(q) = \sum_{k=1}^{M} a_k X_k(q) \tag{10}$$

with

$$X_k(q) = \Delta\rho^2 \int B_k(R) F^2(q,R) dR \tag{11}$$

which demonstrates that this is also a linear problem.

The chi-squared function can be minimized by many different methods, for example by making a qualified guess on the values of the parameters and then simply vary the parameters one by one so that successively lower values of chi-squared are obtained. Such a simple (but time consuming!) *grid search* method would work. It would, however, be better to take advantage of the general properties of the chi-squared function and of the fitting function.

The minimum of chi-squared occurs where the partial derivatives of (1) with respect to a_k are equal to zero:

$$\frac{\partial \chi^2}{\partial a_k} = 0 \qquad \text{for } k = 1,\ldots,M \tag{12}$$

Equations (1) and (3) give:

$$\sum_{i=1}^{N} \frac{1}{\sigma_i^2} \left[I^{\mathrm{exp}}(q_i) - \sum_{j=1}^{M} a_j X_j(q_i) \right] X_k(x_i) = 0 \qquad \text{for } k = 1,\ldots,M \tag{13}$$

which is equivalent to the *normal equations*:

$$\sum_{j=1}^{M} \alpha_{kj} a_j = \beta_k \tag{14}$$

where

$$\alpha_{jk} = \sum_{i=1}^{N} \frac{X_j(q_i) X_k(q_i)}{\sigma_i^2} \tag{15}$$

and

$$\beta_k = \sum_{i=1}^{N} \frac{I^{\exp}(q_i)X_k(q_i)}{\sigma_i^2} \tag{16}$$

In matrix notation

$$\mathbf{A} \cdot \mathbf{a} = \mathbf{b} \tag{17}$$

where $[\mathbf{A}]_{ij} = \alpha_{ij}$ and $[\mathbf{b}]_k = \beta_k$.

The values for a_k that minimize chi-squared is thus determined by solving a set of linear equations. It should be noted [14,19] that the equations should *not* be solved by numerically calculating the inverse matrix and multiplying it on both sides of the equations. If the equations are close to being singular (which is not an unusual situation) the numerical calculations will give an accumulation of round-off errors and the final solution for a_k will *not* fulfill the original equation (17). It is much better to use a more robust method like Gauss–Jordan elimination with pivoting [14,19] for *solving* the equations.

For estimating the errors on a_j a basic rule for accumulation of errors is applied. For the function $f(x_1,...,x_N)$ of the parameters x_i with known errors $\sigma(x_i)$:

$$\sigma^2(f) = \sum_{i=1}^{N} \left(\frac{\partial f}{\partial x_i}\right)^2 \sigma^2(x_i) \tag{18}$$

This equation is valid if the a_js are independent parameters. If the parameters a_j are considered to be functions of the observed intensities $I^{\exp}(q_i)$ so that $a_j(I^{\exp}(q_1),...,I^{\exp}(q_N))$, then

$$\sigma^2(a_j) = \sum_{i=1}^{N} \left(\frac{\partial a_j}{\partial I^{\exp}(q_i)}\right)^2 \sigma_i^2 \tag{19}$$

In order to calculate the quantity in the brackets, the formal mathematical solution to (17) is used:

$$a_j = \sum_{k=1}^{M} [\mathbf{A}^{-1}]_{jk}\beta_k = \sum_{k=1}^{M} [\mathbf{A}^{-1}]_{jk} \sum_{i=1}^{N} \frac{I^{\exp}(q_i)X_k(q_i)}{\sigma_i^2} \tag{20}$$

The derivative of this equation with respect to $I^{\exp}(q_i)$, which in this context is considered to be a parameter, is then calculated:

$$\frac{\partial a_j}{\partial I^{\exp}(q_i)} = \sum_{k=1}^{M} [\mathbf{A}^{-1}]_{jk} \frac{X_k(q_i)}{\sigma_i^2} \tag{21}$$

Inserting this in (19) gives

$$\sigma^2(a_j) = \sum_{k=1}^{M}\sum_{l=1}^{M} [\mathbf{A}^{-1}]_{jk} [\mathbf{A}^{-1}]_{jl} \left[\sum_{i=1}^{N} \frac{X_k(q_i)\, X_l(q_i)}{\sigma_i^2} \right] \tag{22}$$

Noting that $[\mathbf{A}]_{jk} = \alpha_{jk} = \sum_{i=1}^{N} X_j(q_i)\, X_k(q_i)/\sigma_i^2$ the final result is

$$\sigma^2(a_j) = [\mathbf{A}^{-1}]_{jj} \tag{23}$$

which means that the square of the errors are given by the diagonal elements of $\mathbf{A}^{-1}$. If the reduced chi-squared χ_r^2 at the minimum is larger than one, it is common to set

$$\sigma^2(a_j) = \chi_r^2 [\mathbf{A}^{-1}]_{jj} \tag{24}$$

as this to a certain extent takes into account the short-comings of the applied model function and/or systematic errors in the data.

Using (24) the errors on, for example, $p(r)$ can be estimated as

$$\sigma^2[p(r)] = \sum_{k=1}^{M} \sigma^2(a_k) B_k(r)^2 = \chi_r^2 \sum_{k=1}^{M} [\mathbf{A}^{-1}]_{kk} B_k(r)^2 \tag{25}$$

This equation has the short-coming that it assumes that the a_js are independent and thus neglects the covariances of the parameters a_j. Taking this properly into account [14] modifies the expression to

$$\sigma^2[p(r)] = \chi_r^2 \sum_{k=1}^{M}\sum_{l=1}^{M} [\mathbf{A}^{-1}]_{kl} B_k(r) B_l(r) \tag{26}$$

For the indirect Fourier transformation [1] the number of basis functions in Eq. (4) usually has to be quite large (30–60) in order to give a sufficient resolution for $p(r)$. However, this often results in a nearly singular set of equations and large oscillations in $p(r)$. The function is expected to have a relatively smooth behavior, and therefore a smoothness constraint on $p(r)$ is applied. This is done in such a way that the normal equations remain a linear set of equations. The expression $\chi^2 + \lambda N_c$ is minimized instead of χ^2, where N_c is the measure of the smoothness, $N_c = \sum_{j=1}^{M-1} (a_{j+1} - a_j)^2 + a_M^2 + a_1^2$ [1,20], and λ is a constant which can easily be chosen by the point-of-inflection method [1]. Alternative methods for choosing λ can be found in [21].

For determination of size distributions it is physically reasonable to apply a non-negativity constraint for $N(r)$ as well as a smoothness constraint. This can be done by reducing the normal equations in a systematic way, so that only those that give non-negative values are kept. This approach also gives a linear set of equations [22].

The application of the smoothness constraint has in both types of applications the consequence that Eq. (26) cannot be used for a reliable determination of the errors on the distribution functions. It can in these cases be recommended to use the Monte Carlo method [14,19]. In this method a large set of additional 'experimental' data sets (typically $N_{MC} = 50$) are generated from the original data set by adding random errors to the original data sets of the same magnitude as those of the original experimental data. These data sets are analyzed and give the functions $p_i(r)$, $i=1,\ldots, N_{MC}$ and the errors on $p(r)$ are calculated as

$$\sigma^2[p(r)] = \frac{1}{N_{MC}} \sum_{i=1}^{N_{MC}} [p_i(r) - p(r)]^2 \tag{27}$$

This approach automatically takes into account the covariances and it can of course also be used for determining the errors on other parameters derived from a_j. It should be noted that the 'experimental' data only enter the right-hand side of the normal equations. When the Gauss–Jordan elimination procedure is used for solving the equations, the different right-hand sides can be treated simultaneously, and the equations have to be solved only once [19].

Experimental scattering data are always influenced by instrumental smearing, and it may be necessary to include corrections for this in the data analysis. Owing to the finite resolution of the instrument the scattering in a region around the nominal scattering vector $\langle q \rangle$ is probed. For small-angle neutron scattering, the distribution of scattering vectors q can be described by a resolution function $R(\langle q \rangle, q)$ (see, for example Ref. [23]), and the smearing effects can be taken into account in the model scattering intensity by

$$I^{\mathrm{mod}}(\langle q \rangle) = \sum_{k=1}^{M} a_k \tilde{X}_k(\langle q \rangle), \quad \text{where} \quad \tilde{X}_k(\langle q \rangle) = \int R(\langle q \rangle, q)\, X_k(q) dq \tag{28}$$

The experimental data which enter the expression for chi-squared (1) should be written as $I(\langle q_i \rangle)$ as they are recorded for the nominal scattering vectors. For small-angle X-ray scattering data recorded using a long-slit camera, the smearing is calculated using the usual procedure, which involves weighting functions (see, e.g. Ref. [1]). This procedure is numerically more complicated as three integrals have to be calculated, however, the result is in principle the same as described by Eq. (28) as it is the basis functions which are smeared.

In most small-angle neutron scattering experiments, the data are recorded using more than one instrumental setting. Each setting corresponds to a set of values of the wavelength, wavelength resolution, collimation and sample-to-detector distance. Therefore each of the N_{set} settings has its own resolution function $R_j(\langle q \rangle, q)$, and it is therefore convenient to write

$$\chi^2 = \sum_{j=1}^{N_{\mathrm{set}}} \sum_{i=1}^{N(j)} \left(\frac{I_j^{\mathrm{exp}}(\langle q_i \rangle) - I_j^{\mathrm{mod}}(\langle q_i \rangle)}{\sigma_{ji}} \right)^2 \tag{29}$$

where the index j refers to which data set is considered. The model intensity is then

$$I_j^{\mathrm{mod}}(\langle q \rangle) = \sum_{k=1}^{M} a_k \tilde{X}_{kj}(\langle q \rangle), \quad \text{where} \quad \tilde{X}_{kj}(\langle q \rangle) = \int R_j(\langle q \rangle, q)\, X_k(q) dq \tag{30}$$

The corresponding changes to the normal equations ((13)–(16)) consist in changing the summations over $i = 1,\ldots,N$ to a double summations over $j = 1,\ldots,N_{\mathrm{set}}$ and $i = 1,\ldots,N(j)$ and changing q_i to $\langle q_i \rangle$.

It is often so that not all data sets are known on an absolute scale, and furthermore, even if they are, there are typically small (systematic) errors of a few percent in the scale. As the errors from counting statistics can be less than one percent, the errors on the scales are quite important when fitting the data. The scale factors of the data sets should therefore be adjusted. Svergun [24] has suggested a method for adjusting the scale of one data set with respect to another, which is somewhat complicated: the normal equations for the problem without the smoothness constraint plus an extra linear equation for the scale factor are solved by singular value decomposition [25]. However, a simpler approach can also be used [26]. First the most reliable data set is chosen so that the other sets can be scaled to match this one. Then the data sets are scaled so that they agree within 10–25% in the overlap region, and the constant λ is determined by the point-of-inflection method. The value of λ is kept fixed while the scale factors are optimized. It should be noted that it is only the β_ks which depend on the scale factors, and therefore it is not necessary to recalculate (and smear by instrumental resolution) the α_{ij}s and the basis functions which enter β_j. The scale factors can be adjusted relatively fast to an accuracy better than 0.5% by a simple grid search combined with a parabolic approximation of χ^2 close to the minimum [13,26]. If three or more data sets have been recorded it may be necessary to go through the data sets several times and adjust scale factors until the procedure is converged. It can be recommended to determine the scale factors by this procedure before performing least-squares fit using analytical models as it can save a lot of computer time.

2.2 Non-linear Method

If the fitting function is not a linear function of the parameters, the least-squares problem is said to be non-linear. As for the linear method, the chi-squared function can simply be minimized by a grid search in which one makes a qualified guess on the values of the parameters and then successively and repeatedly optimizes the parameters one by one. However, this grid search method is very time consuming and it is often advantageous to apply more advanced methods. Due to the non-linearity of the fitting function all of the methods require a set of starting values for the parameters.

A method, which is better than the grid search and also relatively simple is the *gradient* method also known as the *steepest descent* method [13,14]. In this method one calculates analytically or more often numeri-

cally, the gradient of chi-squared, $\partial\chi^2/\partial a_j$. The search for a new set of parameter values is done along the negative direction of the gradient. All parameters are changed simultaneously and the new values $\mathbf{a}_{new}$ are obtained from the old set $\mathbf{a}_{old}$ by

$$\mathbf{a}_{new} = \mathbf{a}_{old} + \delta\mathbf{a} = \mathbf{a}_{old} + \text{constant} \times \mathbf{b} \tag{31}$$

where $\mathbf{b}$ is the negative gradient ($[\mathbf{b}]_i = -\partial\chi^2(\mathbf{a}_{old})\partial a_i$) and the constant is appropriately chosen, so that χ^2 decreases. The steepest descent method is effective relatively far away from the minimum. As the minimum is approached it becomes gradually more inefficient.

A method which works better close to the minimum is based on a set of equations similar to the normal equations for the linear problem. These equations have to be solved iteratively [13,14]. Let a_i be an estimate of the parameters which is not too far from the minimum of χ^2. A multi-parameter Taylor expansion of chi-squared around $\mathbf{a}$ gives:

$$\chi^2(\mathbf{a}') = \chi^2(\mathbf{a}) + \sum_{i=1}^{M} \frac{\partial\chi^2}{\partial a_i}(\mathbf{a})\,\delta a_i + \frac{1}{2}\sum_{i,j=1}^{M} \frac{\partial^2\chi^2}{\partial a_i \partial a_j}(\mathbf{a})\,\delta a_i\,\delta a_j + \ldots$$
$$\approx c - \mathbf{b}\cdot\delta\mathbf{a} + \frac{1}{2}\,\delta\mathbf{a}\cdot\mathbf{A}\cdot\delta\mathbf{a} \tag{32}$$

where $= \partial\mathbf{a} = \mathbf{a}' - \mathbf{a}$ and

$$c = \chi^2(\mathbf{a}) \quad [\mathbf{b}]_i = -\frac{\partial\chi^2}{\partial a_i}(\mathbf{a}) \quad [\mathbf{A}]_{ij} = \frac{\partial^2\chi^2}{\partial a_i\,\partial a_j}(\mathbf{a}) \tag{33}$$

Using the approximation in the second line of (32) the gradient of χ^2 in $\mathbf{a}'$can be estimated as

$$\frac{\partial\chi^2}{\partial a_i}(\mathbf{a}') = \mathbf{A}\cdot\delta\mathbf{a} - \mathbf{b} \tag{34}$$

For $\mathbf{a}' = \mathbf{a}_{min}$ this gradient is equal to zero and one has the normal equations

$$\mathbf{A}\cdot\delta\mathbf{a} = \mathbf{b} \tag{35}$$

where **A** and **b** are calculated at the old value of **a**. Thus, one obtains (formally) a new estimate for **a** by

$$\mathbf{a}_{\text{new}} = \mathbf{a}_{\text{old}} + \delta\mathbf{a} = \mathbf{a}_{\text{old}} + \mathbf{A}^{-1} \cdot \mathbf{b} \tag{36}$$

This method can be applied successively until the changes in χ^2 are negligible. However, there is one problem in applying this method directly as it requires that both the first order and second order derivatives are available. It is often only practically possible to calculate the derivatives numerically. This is quite time consuming as the calculation of the second order derivative requires the calculation of $M(M-1)/2$ terms and each of these requires the evaluation of the fitting function in N values. It is more efficient [13] to use a first order Taylor expansion of the fitting function $I^{\text{mod}}(q,\mathbf{a})$:

$$I^{\text{mod}}(q;\mathbf{a}') \approx I^{\text{mod}}(q;\mathbf{a}) + \sum_{j=1}^{M} \frac{\partial I^{\text{mod}}(q;\boldsymbol{a})}{\partial a_j} \delta a_j \equiv I^{\text{mod}}(q;\mathbf{a}) + \sum_{j=1}^{M} \delta a_j X_j(q;\mathbf{a}) \tag{37}$$

where $\mathbf{a}' = \mathbf{a} + \delta\mathbf{a}$ and

$$X_j(q;\mathbf{a}) = \frac{\partial I^{\text{mod}}(q;\mathbf{a})}{\partial a_j} \tag{38}$$

Inserting the right-hand-side of (37) in the expression for chi-squared (Eq. (1)), and considering $[I^{\text{exp}}(q) - I^{\text{mod}}(q;\mathbf{a})]$ as the 'experimental' data, it is straight forward to see that the normal equations for δa_j for the linearized function are the same as those for a_j in the linear problem, with $[I^{\text{exp}}(q) - I^{\text{mod}}(q;\mathbf{a})]$ instead of $I^{\text{exp}}(q)$. Hence,

$$\alpha_{jk} = \sum_{i=1}^{N} \frac{X_j(q_i;\boldsymbol{a})\, X_k(q_i;\boldsymbol{a})}{\sigma_i^2} \quad \text{and} \quad \beta_k = \sum_{i=1}^{N} \frac{[I^{\text{exp}}(q) - I^{\text{mod}}(q;\boldsymbol{a})]\, X_k(q_i;\boldsymbol{a})}{\sigma_i^2} \tag{39}$$

where $X_j(q;\mathbf{a}) = \partial I^{\text{mod}}(q;\mathbf{a})/\partial a_j$. A numerical calculation of these derivatives requires only on the order of $M \times N$ calculations.

The method with linearized fitting functions works best close to the minimum of chi-squared, whereas the gradient search is better further away. Ideally, the two methods should be combined, so that the methods

are used in the range where they are best suited. There exists an approach suggested by Marquardt [27] which smoothly combines the two methods. A parameter λ (not to be confused with the prefactor of the smoothness measure in the IFT methods) is used for enhancing the diagonal elements of the matrix $[\mathbf{A}]_{ij} = \alpha_{ij}$ so that the normal equations become

$$\mathbf{A}' \cdot \delta\mathbf{a} = \mathbf{b} \tag{40}$$

with

$$\alpha'_{ij} = \begin{cases} \alpha_{ij}(1+\lambda) & \text{for } i = j \\ \alpha_{ij} & \text{for } i \neq j \end{cases} \tag{41}$$

For λ small, the normal equations are basically unchanged and the method is efficient close to the minimum. For λ large, the normal equations reduce to a set of non-coupled equations:

$$\lambda\alpha_{jj}\,\delta a_j \approx \beta_j \qquad \text{for } j = 1,\ldots,M \tag{42}$$

which have the solutions

$$\delta a_j \approx \frac{1}{\lambda\alpha_{jj}}\,\beta_j \tag{43}$$

Noting that β_j is the negative gradient, a comparison with Eq. (31) shows that the method in this case is the same as the steepest descent method with the constant equal to $1/(\lambda\alpha_{jj})$. Chi-squared will always decrease for sufficiently large values of λ. The character of the search method is thus determined by the value of λ, and λ should be large far away from the minimum and small close to the minimum. Marquardt [27] has designed the following procedure:

1. Calculate $\chi^2(\mathbf{a})$.
2. Set $\lambda = 0.001$.
3. Calculate $\mathbf{A}$ and $\mathbf{b}$.
4. Calculate $\mathbf{A}'$ for the current λ and determine $\delta\mathbf{a}$.
5. If $\chi^2(\mathbf{a} + \delta\mathbf{a}) > \chi^2(\mathbf{a})$, multiply λ by 10 and repeat (4).
6. If $\chi^2(\mathbf{a} + \delta\mathbf{a}) < \chi^2(\mathbf{a})$, divide λ by 10, take $\mathbf{a} + \delta\mathbf{a}$ to be the current $\mathbf{a}$ and repeat (3).

The iterations are continued until the decrease of χ^2 becomes negligible. It should be noted that the normal equations, as for the linear problem, should be solved using a numerically stable method like the Gauss–Jordan elimination procedure [14].

The standard errors on the parameters a_j can be estimated as for the linear problem:

$$\sigma(a_j) = \chi_r^2 [\mathbf{A}^{-1}]_{jj} \tag{44}$$

However, this method only works if the fitting function is not strongly non-linear and if the parameters are not strongly correlated. Another and more reliable approach is to determine $\sigma(a_j)$ as the value for which chi-squared increases by one, when a_j is fixed at $a_j + \sigma(a_j)$ and the other parameters are optimized [13]. If the reduced chi-squared is not equal to one for the optimum values of the parameters, the increase in chi-squared should be taken as χ_r^2 at the minimum instead of one. The advantage of this method is that it takes into account the correlation between the parameters.

It should be noted that the method by Marquardt [27] for optimizing chi-squared may not work for highly non-linear fitting functions with significant correlations between the fitting parameters. For such problem it can be recommended to use the simple grid search in which the parameters are optimized one by one repeatedly. This approach has the advantage that it always works although it is very time consuming. The grid search may be able to bring the parameter values sufficiently close to the optimum values, that the method of Marquardt can be used.

The instrumental smearing effects should, as discussed for the linear problem, be included in the calculation of the model function. For X-ray scattering in the long-slit geometry this is done using the weighting functions [28] and performing three numerical integrations. This is quite time-consuming and makes it difficult to perform fits of complicated model functions.

For small-angle neutron scattering the model function can be written as

$$I^{\mathrm{mod}}(\langle q \rangle) = \int R(\langle q \rangle, q) \, \frac{d\sigma(q)}{d\Omega} \, dq \tag{45}$$

where $d\sigma(q)/d\Omega$ is the ideal scattering intensity (the cross section, see next section), and $R(\langle q \rangle, q)$ is the resolution function described in the

previous section. If several instrumental settings have been used for recording the data, this of course has to be taken into account.

The actual calculation of the integral in (45) is done numerically. For small-angle neutron scattering experiments, the resolution function is well approximated by a Gaussian function [23,29,30] and only about 10 points is required for calculating the integral. In an efficient implementation [31] the resolution function is calculated once and for all in the beginning of the program, and saved for later use. In this way unnecessary repeated calculations are avoided. It should also be noted that although only 10 points are required in the convolution, it means that the cross section should be evaluated for $10 \times N$ values, where N is the number of measured points. If the expressions for the cross section are complex, the calculation times can be greatly reduced by making use of master curves and interpolations [29].

3. Models

In this section some of the most common expressions for form factors and structure factors will be reviewed. It is impractical to give all the mathematical expressions in the present notes, and for some of the models only the references to the original papers are given. The reader is encouraged always to look into the original papers in order to check the range of validity of the expressions (and for checking for possible typing errors in the present notes).

The differential scattering cross section $d\sigma(q)/d\Omega$ of a sample can be defined as the number of scattered neutrons or photons per unit time, relative to the incident flux of neutron or photons, per unit solid angle at q per unit volume of the sample. The flux is the number of neutron or photons per unit time and per unit area at the sample position. It is convenient to use the cross section as it does not depend on the form or transmission of the sample.

For a mono-disperse collection of (spherically symmetric) particles the scattering cross section can be written as

$$\frac{d\sigma(q)}{d\Omega} = n\Delta\rho^2 V^2 P(q) S(q) \tag{46}$$

where n is the number density of particles, $\Delta\rho$ is the difference in scattering length density between the particles and the solvent/matrix,

V is the volume of the particles, $P(q)$ is the particle *form factor* and $S(q)$ is the *structure factor*. The form factor describes the structure of the particles and fulfils $P(q = 0) = 1$. The structure factor describes the interference of scattering from different particles and contains information on the interaction between the particles. For very dilute systems $S(q) = 1$ and the structure factor can be neglected.

An alternative approach is to define the cross section per unit mass of solute instead of per unit volume of the sample. This cross section can be written as

$$\frac{d\sigma_m(q)}{d\Omega} = \frac{1}{M} \Delta\rho_m^2 M^2 P(q)S(q) = \Delta\rho_m^2 MP(q)S(q) \tag{47}$$

where M is the molecular mass of a particle and $\Delta\rho_m$ is the scattering length difference per unit mass of the solute. The factor $1/M$ is the number of particles per unit mass of solute.

The above expressions [46,47] implicitly assume spherical symmetry of the particle shape and the interactions. For anisotropic identical particles the cross section is

$$\frac{d\sigma(q)}{d\Omega} = \Delta\rho^2 V^2 \left[\sum_i F_i(q,\mathbf{e}_i)^2 + \sum_{i,j} F_i(q,\mathbf{e}_i) F_j(q,\mathbf{e}_j) S_{i,j}(q, \mathbf{e}_i, \mathbf{e}_j) \right] \tag{48}$$

where the sums are over all particles in the sample and $F_i(q,\mathbf{e}_i)$ is the amplitude of the form factor for the ith particle with orientation given by the unit vector $\mathbf{e}_i$. The $S_{ij}(q,\mathbf{e}_i,\mathbf{e}_j)$ functions are the partial structure factors which depend on orientations. Note that the first term in Eq. (48) is just the orientational averaged form factor: $P(q) \equiv \langle F^2(q) \rangle_0$.

For particles with only a small anisotropy, it can be assumed that the interactions are independent of the orientation and given by the average size of the particles. This leads to the *decoupling approximation* [32].

$$\frac{d\sigma(q)}{d\Omega} = \Delta\rho^2 V^2 P(q)[1 + \beta(q)(S(q) - 1)] \tag{49}$$

where

$$\beta(q) = \langle F(q) \rangle_0^2 / \langle F^2(q) \rangle_0 \tag{50}$$

and $S(q)$ is the structure factor calculated for the average particle size.

For polydisperse systems it is also not possible to write the scattering cross section as product of a form factor and a structure factor. In this case the scattering cross section has the form:

$$\frac{d\sigma(q)}{d\Omega} = \Delta\rho^2 \left[\int_0^\infty D(R)\, V(R)^2\, F(q,R)^2\, dR + \int_0^\infty \int_0^\infty D(R)V(R)D(R')V(R')F(q,R)F(q,R')S(R,R',q)dRdR' \right] \tag{51}$$

where $D(R)$ is the number size distribution, $V(R)$ is the volume of a particle with radius R and form factor $F(q,R)$, and $S(R,R',q)$ are partial structure factors.

For systems with small polydispersities, a decoupling approach similar to the one for anisotropic particles [32] can be used. It is assumed that interactions are independent of size. With this one obtains:

$$\frac{d\sigma(q)}{d\Omega} = \Delta\rho^2 \langle V^2 P(q) \rangle \, [1 + \beta(q)(S(q) - 1)] \tag{52}$$

where $\langle V^2 P(q) \rangle = \int D(R)V(R)^2 F(q,R)^2 dR$ and

$$\beta(q) = \left[\int D(R)V(R)F(q,R)dR \right]^2 / \left[\int D(R)V(R)^2 F(q,R)^2 dR \right] \tag{53}$$

and $S(q)$ is the structure factor calculated for the average particle size. Note that Eqs. (51,52) can also be used for slightly anisotropic particles, if $F_i(q,R)$ is replaced by $\langle F_i(q,R) \rangle_0$ and $F_i(q,R)^2$ is replaced by $\langle F_i(q,R)^2 \rangle_0$.

It is also possible to use a *local monodisperse approximation* for including the effects of polydispersity [7]. In this approach it is assumed that a particle of a certain size is always surrounded by particles with the same size. Following this the scattering is approximated by that of monodisperse sub-systems weighted by the size distribution:

$$\frac{d\sigma(q)}{d\Omega} = \Delta\rho^2 \int D(R)V(R)^2 F(q,R)^2 S(q,R) dR \tag{54}$$

in which it has been indicated that the structure factor is for particles of size R. This approach works better than the decoupling approximation (52) for systems with larger polydispersities and higher concentrations.

3.1. Form Factors

In the following it will be assumed that the particles are randomly oriented in the sample so that the theoretical form factors for anisotropic particles have to be averaged over orientation. Note that for spherical objects the form factor can be written as $P(q) = F^2(q)$, where $F(q)$ is the amplitude of the form factor.

(1) Homogeneous sphere

The form factor of a homogeneous sphere was calculated already in 1911 by Lord Rayleigh [33]. For a sphere with radius R:

$$F_1(q,R) = \frac{3[\sin(qR) - qR\cos(qR)]}{(qR)^3} \tag{55}$$

(2) Spherical shell

This form factor is obtained by subtracting the empty core with a proper weighting by the volumes:

$$F_2(q) = \frac{V(R_1)F_1(q,R_1) - V(R_2)F_1(q,R_2)}{V(R_1) - V(R_2)} \tag{56}$$

where $V(R) = 4\pi R^3/3$ and R_1 and R_2 are the outer and inner radius of the shell, respectively. An infinitely thin shell with radius R has the form factor $F_2(q)' = \sin(qR)/(qR)$.

(3) Spherical concentric shells

This form factor is a generalization of the shell form factor. Let R_i, $i = 1,N$ be the radii of the shells and ρ_i be their scattering densities. With this:

$$F_3(q) = \frac{1}{M_3}\left[\rho_1 V(R_1)F_1(q,R_1) + \sum_{i=2}^{N}(\rho_i - \rho_{i-1})V(R_i)F_1(q,R_i)\right] \tag{57}$$

where M_3 is the scattering mass or scattering volume of the particle, given by:

$$M_3 = \rho_1 V(R_1) + \sum_{i=2}^{N} V(R_i)(\rho_i - \rho_{i-1}) \tag{58}$$

(4) Particles consisting of spherical subunits

The expression was derived by Debye in 1915 [34]. For a particle consisting of P subunits:

$$P_4(q) = \frac{1}{M_4^2} \sum_{i,j=1}^{P} M_3(i)\, M_3(j)\, F_3(q,i)\, F_3(q,j) \frac{\sin(qr_{ij})}{qr_{ij}} \tag{59}$$

where $F_3(q,i)$ and $M_3(i)$ are the form factor and scattering mass of the ith particle, respectively. r_{ij} is the distance between the centers of the ith and the jth subunit, and

$$M_4 = \sum_{i=1}^{P} M_3(i) \tag{60}$$

(5) Ellipsoid of revolution

This expression was determined by Guinier [35]. The averaging over orientations has to be done numerically. For the semi axes $R,R,\varepsilon R$:

$$P_5(q,R,\varepsilon) = \int_0^{\pi/2} F_1^2[q,r(R,\varepsilon,\alpha)] \sin\alpha \, d\alpha \tag{61}$$

where $r(R,\varepsilon,\alpha) = R(\sin^2\alpha + \varepsilon^2\cos^2\alpha)^{1/2}$. It is straight forward to generalize (61) for concentric elliptical shells. $F_1(q,r)$ has to be replaced by $F_3(q)$ in which the volumes are $V(R) = 4\pi\varepsilon R^3/3$. Note, that the different shells can have different values of ε. The form factor of an infinitely thin elliptical shell is given by (61) with $F_1(q,r)$ replaced by $F_2(qr)'$.

(6) Tri-axial ellipsoid

For this object two numerical integrations have to be performed in order to get the orientational average. For the semi axes a,b,c [36]:

$$P_6(q,a,b,c) = \frac{2}{\pi} \int_0^{\pi/2} \int_0^{\pi/2} F_1^2[q,r(a,b,c,\alpha,\beta)] \sin\alpha \, d\alpha \, d\beta \tag{62}$$

where $r(a,b,c,\alpha,\beta) = [(a^2 \sin^2\beta + b^2\cos^2\beta) \sin^2\alpha + c^2\cos^2\alpha]^{1/2}$. The form factor for the tri-axial ellipsoid can be generalized in the same way as (61) for tri-axial ellipsoids consisting of concentric shells. The form factor of an infinitely thin elliptical shell is given by (62) with $F_1(q,r)$ replaced by $F_2(qr)'$.

(7) Cube and rectangular parallelepipedons

Two orientational averages have to be performed. For the edge lengths a,b,c [37]:

$$P_7(q,a,b,c) = \tag{63}$$

$$\frac{2}{\pi} \int_0^{\pi/2} \int_0^{\pi/2} \frac{\sin(qa \sin\alpha \cos\beta)}{qa \sin\alpha \cos\beta} \frac{\sin(qb \sin\alpha \cos\beta)}{qb \sin\alpha \sin\beta} \frac{\sin(qc \cos\alpha)}{qc \cos\alpha} \sin\alpha \, d\alpha \, d\beta$$

(8) Truncated octahedra

The equations for an oriented particle were given by Hendricks, Schelten and Schmatz [38]. The orientational average has to be done as in Eq. (63).

(9) Faceted sphere

The equations for an oriented particle were given by Dubey [39] (see also Ref. [40]). The orientational average has to be done as in Eq. (63).

(10) Cube with terraces

The equations for an oriented particle were given by Rodríguez, Gómez Sal, Moreno, de Geyer, and Janot [41]. The orientational average has to be done as in Eq. (63).

(11) Cylinder

The expression for a cylinder with radius R and length L was given by Fournet [42].

$$P_{11}(q) = \int_0^{\pi/2} \left[\frac{2B_1(qR \sin\alpha)}{qR \sin\alpha} \frac{\sin((qL \cos\alpha)/2)}{(qL \cos\alpha)/2} \right]^2 \sin\alpha \, d\alpha \tag{64}$$

where $B_1(x)$ is the first order Bessel function. An expression for cylinders consisting of concentric shells can be constructed by an approach similar to the one used for spherical particles. The form factor of an infinitely thin cylindrical shell with closed ends is given by (64) with the terms in the square brackets replaced by $2B_0(q\ R \sin\alpha) \cos[(qL \cos\alpha)/2]$.

(12) Cylinder with elliptical cross section

This expression was given by Mittelbach and Porod [43] for a cylinder of length L and with cross-section semi axes a and b:

$$P_{12}(q) = \frac{2}{\pi} \int_0^{\pi/2} \int_0^{\pi/2} \left[\frac{2B_1(qr(a,b,\phi,\alpha)}{qr(a,b,\phi,\alpha)} \frac{\sin((qL\cos\alpha)/2)}{((qL\cos\alpha)/2)} \right] d\phi \sin\alpha\, d\alpha \qquad (65)$$

where $r(a,b,\phi,\alpha) = [a^2\sin^2\phi + b^2\cos^2\phi]^{1/2} \sin\alpha$. An expression for cylinders consisting of concentric shells with elliptical cross section can be constructed by an approach similar to the one used for spherical particles and for tri-axial ellipsoids. The shells can have varying eccentricities (a/b).

(13) Cylinder with spherical end-caps

The equations were given by Cusack [44]. Expressions for a shell particle were also given.

(14) Infinitely thin rod

The expression was determined by Neugebauer [45]:

$$P_{14}(q) = 2\mathrm{Si}(qL)/(qL) - 4\sin^2(qL/2)/(q^2L^2) \qquad (66)$$

where

$$\mathrm{Si}(x) = \int_0^x t^{-1} \sin t\, dt \qquad (67)$$

and L is the length.

(15) Infinitely thin circular disk

The expression was determined by Kratky and Porod [46]:

$$P_{14}(q) = \frac{2}{q^2R^2}\left[1 - \frac{B_1(2qR)}{qR}\right] \qquad (68)$$

where R is the radius of the disk.

(16) Fractal aggregates

An empirical expression for a mass fractals consisting of spheres with a radius R has been given by Teixeira [47]:

$$P_{16}(q) = \left[1 + \frac{1}{(qR)^D} \frac{D\Gamma(D-1)}{[1+1/(q^2\xi^2)]^{(D-1)/2}} \sin[(D-1)\tan^{-1}(q\xi)]\right] F_1^2(q) \quad (69)$$

where D is the fractal dimension, ξ is a cut-off length for the fractal correlations, and $\Gamma(x)$ is the gamma function. (Note that expressions for fractal surfaces have been given by Bale and Schmidt [48].)

(17) Flexible polymers with Gaussian statistics

Flexible polymer chains which are not self-avoiding obey Gaussian statistics. Debye [49] has calculated the form factor of such chains:

$$P_{17}(q) = 2[\exp(-u) + u - 1]/u^2 \quad (70)$$

with $u = \langle R_g^2 \rangle q^2$, where $\langle R_g^2 \rangle$ is the ensemble average radius of gyration squared: $\langle R_g^2 \rangle = (Lb)/6$, where L is the contour length and b is the statistical (Kuhn) segment length.

(18) Flexible self-avoiding polymers

Empirical expressions have been given by Utiyama, Tsunashima and Kurata [50]. The parameters should be taken as $\varepsilon = 0.176$, $t = 2/(1-\varepsilon)$, and $s = 2.90$ (see Ref. [51] which also contains a simple approximation).

(19) Semi-flexible polymers without self-avoidance

Numerical interpolation formulae for the Kratky–Porod model [52] have been given by Yoshizaki and Yamakawa [53]. These have recently been corrected using results from Monte Carlo simulations [51].

(20) Semi-flexible polymers with self-avoidance

Numerical interpolation formulae have been given by Pedersen and Schurtenberger [51]. The results are given for $R/b = 0.1$, where R is the cross section radius and b is the Kuhn length. This corresponds to a reduced binary cluster integral of 0.3, which is similar to the value found for polystyrene in a good solvent.

(21) Star polymer with Gaussian statistics

The expression was given by Benoit [54]. For a star with f arms:

$$P_{21}(q) = \frac{2}{fv^2}\left[v - [1 - \exp(-v)] + \frac{f-1}{2}[1 - \exp(-v)]^2\right] \tag{71}$$

with $v = u^2 f/(3f-2)$, and $u = \langle R_g^2 \rangle q^2$, where $\langle R_g^2 \rangle$ is the ensemble average radius of gyration squared of an arm.

(22) Star-burst polymer with Gaussian statistics

Expressions have been given by Burchard and Kajiwara [55] and by Hammouda [56]. The results are obtained by summation of geometrical series. However, it cannot be recommended to use these as the performance of the sums introduces singularities. It is better to use the expressions *before* the sums are performed [57].

(23) Regular comb polymer with Gaussian statistics

Expressions have been given by Casassa and Berry [58].

(24) Arbitrarily branched polymers with Gaussian statistics

The form factor for P subchains can be written as [57]:

$$P_{24}(q) = \frac{1}{M_{24}^2}\left[\sum_{i=1}^{P} \rho_i^2 P_{17}(q,L_i) + 2\sum_{i>j}^{P} \rho_i \rho_j \psi(q,L_i)\psi(q,L_j)\exp(-q^2 d_{ij}^2)\right] \tag{72}$$

where $\langle R_g \rangle$ in $P_{17}(q,L_i)$ is calculated for L_i, the contour length of the ith subchain. ρ_i is the total excess scattering length of the ith subchain. Furthermore,

$$\psi(q,L_i) = [1 - \exp(-u)]/u \tag{73}$$

where $u = \langle R_g^2 \rangle q^2$. The parameter $d_{ij}^2 = L_{ij} b$, where L_{ij} is the separation in contour length between the starting points of the ith and the jth subchains. The scattering mass M_{24} is given by $M_{24} = \sum_{i=1}^{P} \rho_i$.

(25) Sphere with Gaussian chains attached

The expressions have recently been derived by Pedersen and Gerstenberg [59]. For a sphere with radius R and total excess scattering length ρ_s with N_c attached chains of contour length L:

$$P_{25}(q) = \frac{1}{M_{25}^2}\Big[\rho_s^2 F_1^2(q,R) + N_c\rho_c^2 P_{17}(q,L) + N_c(N_c-1)\rho_c^2 S_{cc}(q) + 2N_c\rho_s\rho_c S_{sc}(q)\Big] \quad (74)$$

with:

$$S_{sc}(q) = F_1(q,R)\psi(q,L)\frac{\sin(qR)}{qR} \quad (75)$$

and

$$S_{cc}(q) = \psi(q,L)^2\left[\frac{\sin(qR)}{qR}\right]^2 \quad (76)$$

The scattering mass is: $M_{25} = \rho_s + N_c\rho_c$, where ρ_c is the total excess scattering length of a single chain.

For non-penetrating chains and $R >> R_g$, the form factor is approximately given by Eq. (74) with R in Eqs. (75,76) replaced $R + R_g$ in the $\sin(x)/x$ terms. (R_g is the root-mean-square radius of gyration of a chain.)

(26) Ellipsoid with Gaussian chains attached

An ellipsoid of revolution is considered with radius R, eccentricity ε, and total excess scattering length ρ_e with N_c chains of contour length L and total excess scattering length ρ_c. The form factor is [57]:

$$P_{26}(q) = \frac{1}{M_{26}^2}\Big[\rho_e^2 F_5^2(q,R) + N_c\rho_c^2 P_{17}(q,L) + N_c(N_c-1)\rho_c^2 S_{cc}^{ell}(q) + 2N_c\rho_s\rho_e S_{sc}^{ell}(q)\Big] \quad (77)$$

with:

$$S_{sc}^{ell}(q) = \psi(q,L)\int_0^{\pi/2} F_1[q,r(R,\varepsilon,\alpha)]\frac{\sin[qr(R,\varepsilon,\alpha)]}{qr(R,\varepsilon,\alpha)}\sin\alpha\, d\alpha \quad (78)$$

and

$$S_{cc}^{ell}(q) = \psi(q,L,b)^2\int_0^{\pi/2}\left[\frac{\sin[qr(R,\varepsilon,\alpha)]}{qr(R,\varepsilon,\alpha)}\right]^2\sin\alpha\, d\alpha \quad (79)$$

where $r(R,\varepsilon,\alpha) = R(\sin^2\alpha + \varepsilon^2\cos^2\alpha)^{1/2}$ and $M_{26} = \rho_e + N_c\rho_c$ is the total scattering mass.

For non-penetrating chains and R and $R\varepsilon >> R_g$, the form factor is approximately given by Eq. (77) with $r(R,\varepsilon,\alpha)$ in Eqs. (78,79) replaced by $r(R,\varepsilon,\alpha) + R_g$ in the $\sin(x)/x$ terms.

(27) Cylinder with Gaussian chains attached

A cylinder is considered with radius R, length L_{cyl}, and total excess scattering length ρ_{cyl} with N_c chains of contour length L and total excess scattering length ρ_c. The form factor is [57]:

$$P_{27}(q) = \frac{1}{M_{27}^2}\left[\rho_{cyl}^2 F_{11}^2(q,R) + N_c\rho_c^2 P_{17}(q,L) + N_c(N_c-1)\rho_c^2 S_{cc}^{cyl}(q) + 2N_c\rho_c p_{cyl} S_{sc}^{cyl}(q)\right] \quad (80)$$

with:

$$S_{sc}^{cyl}(q) = \psi(q,L) \times \quad (81)$$

$$\int_0^{\pi/2} \frac{2B_1(qR\sin\alpha)}{qR\sin\alpha} \frac{\sin[(qL\cos\alpha)/2]}{(qL\cos\alpha)/2)} 2B_0(qR\sin\alpha)\cos[(qL\cos\alpha)/2]\sin\alpha\, d\alpha$$

and

$$S_{cc}^{cyl}(q) = \psi(q,L,b)^2 \int_0^{\pi/2} \left\{2B_0(qR\sin\alpha)\cos[(qL\cos\alpha)/2]\right\}^2 \sin\alpha\, d\alpha \quad (82)$$

The scattering mass is: $M_{27} = \rho_{cyl} + N_c\rho_c$.

For non-penetrating chains and R and $L >> R_g$, the form factor is approximately given by Eq. (80) with R replaced by $R + R_g$ and L replaced by $L + 2R_g$ in the $B_0(x)\cos(y)$ terms in Eqs. (81,82).

3.2. Structure factors

There are only very few cases for which the structure factor can be calculated analytically. Most of the available results have been obtained from liquid state theory for particles with spherical symmetry interacting with a spherically symmetric potential. The liquid state theory combines the Ornstein–Zernike integral equation with an approximate closure relation that relates the interaction potential to the direct

correlation function (see e.g. Ref. [60]). If the equations cannot be solved analytically, it is possible to obtain numerical results for the structure factor. In this case a closure relation can be chosen which gives thermodynamically self-consistent results [61,62].

(1) Hard-sphere potential

The particles interact with the hard-sphere radius R_{HS} and have a hard-sphere volume fraction η. The expressions for $S(q)$ have been calculated with the Percus–Yevick approximation for the closure relation (see e.g. [63]):

$$S_1(q) = \frac{1}{1 + 24\eta G(R_{HS}\, q)\ /(R_{HS}\, q)} \tag{83}$$

In this equation:

$$\begin{aligned} G(A) = {} & \alpha(\sin A - A\cos A)/A^2 \\ & + \beta(2A\sin A + (2 - A^2)\cos A - 2/A^3 \\ & + \gamma\left[-A^4\cos A + 4\{(3A^2 - 6)\cos A + (A^3 - 6A)\sin A + 6\}\right]/A^5 \end{aligned} \tag{84}$$

and

$$\begin{aligned} \alpha &= (1 + 2\eta)^2\ /(1 - \eta)^4 \\ \beta &= -6\eta(1 + \eta/2)^2\ /(1 - \eta)^2 \\ \gamma &= \eta\alpha\ /2 \end{aligned} \tag{85}$$

(2) Sticky hard-sphere potential

The model was introduced by Baxter [64]. The particles have a hard-sphere radius R_{HS} and a delta function attractive potential at the surface. The stickiness of the particles is given by the parameter τ. The expressions for the structure factor can be calculated with the Percus–Yevick approximation for the closure relation (see for example, [65,66]). For a hard-sphere volume fraction η and $\kappa = 2qR_{HS}$

$$S_2(q) = \frac{1}{A^2 + B^2} \tag{86}$$

where

$$A = 1 + 12\eta \left\{ \alpha \frac{(\sin \kappa - \kappa \cos \kappa)}{\kappa^3} + \beta \frac{(1 - \cos \kappa)}{\kappa^2} - \frac{\lambda}{12} \frac{\sin \kappa}{\kappa} \right\}$$

and

$$B = 12\eta \left\{ \alpha \frac{(\kappa^2/2 - \kappa \sin \kappa + 1 - \cos \kappa)}{\kappa^3} + \beta \frac{(\kappa - \sin \kappa)}{\kappa^2} - \frac{\lambda}{12} \frac{(1 - \cos \kappa)}{\kappa} \right\}$$

Furthermore,

$$\lambda = \mathrm{Min} \left| 6[\tau/\eta + 1/(1-\eta)] \pm \{36[\tau/\eta + 1/(1-\eta)]\}^{1/2} \right|$$

$$\mu = \lambda\eta(1 - \eta)$$

$$\alpha = \frac{(1 + 2\eta - \mu)}{(1 - \eta)^2} \tag{87}$$

$$\beta = \frac{(-3\eta + \mu)}{2(1 - \eta)^2}$$

(3) Screened Coulomb potential

The particle interaction is described by the hard-sphere radius R_{HS} and an interaction potential given by:

$$V(r) = \frac{C_B Z^2}{(1 + \kappa R_{HS})^2} \frac{\exp[-\kappa(r - 2R_{HS})]}{r} \tag{88}$$

for $r > 2R_{HS}$. $C_B = e^2/(4\pi\varepsilon)$, where ε is the permittivity of the solvent, e the elementary charge, Z the number of charges per particle, and κ is the inverse Debye–Hückel length.

The structure factor has been calculated in the Mean-Spherical Approximation (MSA) and the expressions can be found in Ref. [67]. The results work well for high to medium concentrations, but the pair correlation function becomes unphysical for low concentrations. A better result is obtained by a rescaling of the hard-sphere radius as described by Hansen and Hayter [68]. This procedure is known as the Rescaled MSA (RMSA).

It is also possible to obtain structure factors from thermodynamically self-consistent approaches [60,61,69]. However, these have the problem that the integral equations have to be solved numerically (and iteratively) and this makes the applications quite time consuming.

(4) Hard-sphere potential, polydisperse system

Vrij [70] has given a solution for polydisperse hard spheres for an arbitrary size distribution. It is relatively straight forward to implement it in a computer program, as it only requires the calculation of certain averages of products of form factors and trigonometric functions weighted by the size distribution. The expressions can be found in the paper by Vrij.

(5) Sticky hard-sphere potential, polydisperse system

A solution within the Percus–Yevick approximation has been given by Robertus, Phillipse, Joosten and Levine [71]. This solution is for arbitrary size distributions. In order to obtain the solution a set of equations quadratic in the parameters have to be solved numerically.

(6) Screened Coulomb potential, polydisperse system

The solution in the MSA has been given by Blum and Hoye [72] and Blum [73]. Ruiz-Estrada, Medina-Noyola and Nängele [74] have given a procedure for making a computer implementation using the rescaled mean-spherical approximation.

The implementation of a thermodynamically self-consistent (numerical) approach based on the closure relation of Rogers and Young [61] has been described by D'Aguanno and Klein [60,75].

(7) Cylinders

The scattering can be calculated in the random phase approximation (RPA) [76]. The structure factor for cylinders of length L and radius R, with $L >> R$ is [77]:

$$\left(\frac{d\sigma(q)}{d\Omega}\right)_{\perp} = n\rho_{cyl}^2 \frac{P_{11}(q)}{(1 + \nu P_{11}(q))} \tag{89}$$

where ν is proportional to the concentration of the cylinders, ρ_{cyl} is the total scattering length of a cylinder, and n is the number density.

(8) Solutions of polymers

The scattering can be calculated in the random phase approximation (RPA). The structure factor is [76,78]:

$$\left(\frac{d\sigma(q)}{d\Omega}\right)_S = n\rho_c^2 \frac{P_{17}(q)}{(1 + \nu P_{17}(q))} \tag{90}$$

where ν is proportional to the polymer mass concentration, to the contour length and to the strength of the excluded volume interaction. ρ_c is the total scattering length of a chain. The RPA is only a good approximation for high polymer concentrations. At lower concentrations, it can be recommended to use Eq. (90) with $P_{17}(q)$ replaced by $P_{18}(q)$, and with the parameters normalized, so that Eq. (90) gives the forward scattering (intensity at $q = 0$) and the correlation length predicted by renormalization group theory [79].

4. An application: block copolymer micelles

In this section an example of an application is given. It involves both indirect Fourier transformation, square-root deconvolution, modeling, and least-squares optimization of a model. Both neutron and X-ray small-angle scattering (SANS/SAXS) data are discussed.

The example concerns a block copolymer in a solvent. It is a tri-block and consists of two end blocks of poly(ethylene oxide) (PEO) and a central block of poly(propylene oxide) (PPO). The composition is $EO_{25}PO_{40}EO_{25}$ and the molecular weight is 4500 Da. The molecular weights are 2300 Da for the PPO part and 1100 Da for each of the PEO parts. The polymer is commercially available from Serva AG, Heidelberg, Germany, under the name P85.

The aggregation behavior of P85 in water has been studied by SANS [59,80] and SAXS [81]. The P85 is present as single chains at low temperatures ($T < 5$°C) and forms aggregates/micelles at higher temperatures. This behavior is ascribed to the properties of PPO, which is hydrophilic at room temperatures and becomes hydrophobic at higher temperatures. The PEO is reasonably soluble for temperatures up to $T = 70$°C. The present discussion is limited to the dilute region with well-defined micelles, where the structure factor effects are small.

Measurements on a 0.5% wt. solution at $T = 50$°C were performed at the SANS instrument at Risø National Laboratory [82]. In order to enhance the contrast and reduce the incoherent background, D_2O was used as the solvent. SAXS data have been recorded for a 1% wt. solution $T = 50$°C by a conventional Kratky camera (see, e.g. Ref. [82]) by Glatter

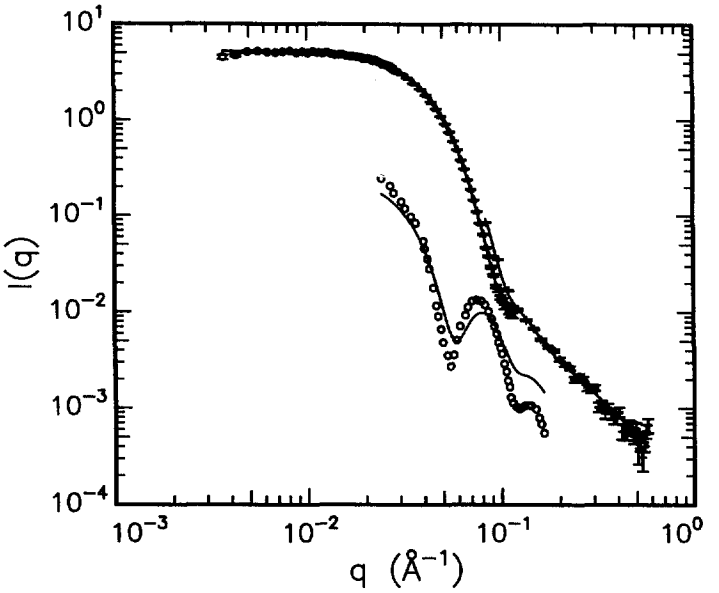

Fig. 1. The small-angle neutron scattering data of 0.5% P85 in D_2O (upper data) [59]. The curve is the fit by the analytical model including polydispersity of the micelles. Note that the fitted curve is discontinuous where the data from different settings overlap due to the instrumental smearing. The lower data are SAXS results on similar micelles [81]. The curve is calculated for the results determined by fitting the SANS data.

et al. [81]. The SAXS data were corrected for instrumental smearing effects in connection with an indirect Fourier transformation as described in Section 2. The desmeared SAXS scattering curve is shown in Fig. 1 together with the SANS data. Note that the SANS data have been recorded using three different instrumental settings. Due to the different smearing effects for the different settings, the data do not coincide in the overlap regions.

The SANS and SAXS scattering curves are remarkably different. The SANS data have a smooth decrease with increasing q and resemble the scattering form factor of a sphere. However, no oscillations are observed (c.f. Eq. (55)). A q^{-2} scattering is observed at large q, which is similar to the scattering from flexible chains obeying Gaussian statistics (c.f. Eq. (70)). In contrast to the the SAXS data have large oscillations. The range of scattering vectors is not large enough to identify power law scattering at large q.

An indirect Fourier transformation of the data sets have been performed [57,81], and the resulting distance distribution functions are

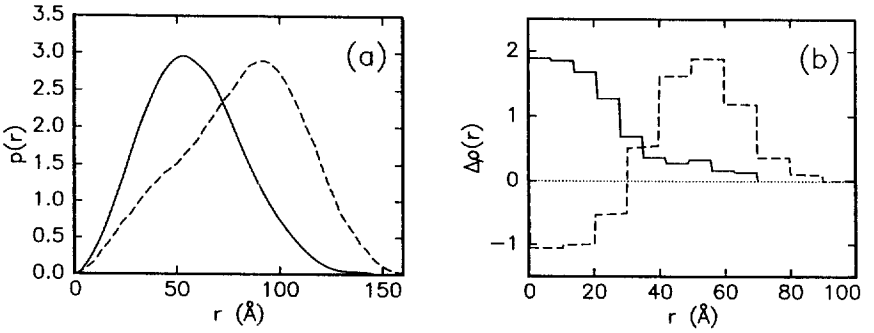

Fig. 2. (a) Distance distribution functions for the data shown in Fig. 1. The full curve is for the SANS data [57] and the broken curve is for the SAXS data [81]. (b) Excess scattering length density distributions for the data shown in (a). The notation is the same as in (a).

shown in Fig. 2(a). Corrections for instrumental resolution effects were included as described in Section 2.1. For the SANS data the file scale factors were also adjusted. The SANS $p(r)$ function has a bell shape with maximum at 55 Å and a tail at larger r, which extends up to about 140 Å. The shape is characteristic for homogeneous almost spherical particles. In contrast to the neutron $p(r)$ function, the SAXS $p(r)$ function has maximum around 90 Å and a much more asymmetric triangular shape, which is characteristic for spherical shell shapes. Thus, the neutrons 'see' a homogeneous particle, whereas the X-rays 'see' a shell. This can be explained by the quite different interaction of X-rays and neutrons with matter. The neutrons are interacting with the nuclei, whereas X-rays are interacting with the electrons. For neutrons the scattering length of hydrogen and deuterium is quite different and the contrast is provided by the difference in deuterium density. It turns out that the polymer has a scattering length density close to zero whereas D_2O has a large scattering length density: the scattering is basically from the 'holes' made by the polymer in the D_2O. For X-rays the contrast is due to the difference in electron density. Organic polymers have electron densities which are quite close to the electron density of water. Therefore, the contrasts are very sensitive to the actual value of the specific volume of the polymer. It seems reasonable from the $p(r)$ functions alone to assume that the specific volumes are so that mainly a shell of dissolved PEO chains is probed. Accurate density measurements [83] as a function of temperature for a series of PEO–PPO–PEO block copolymers can be used for calculating the specific volumes of PEO and PPO

parts. Such calculations [59] show that the contrast of the PPO is small and negative, whereas the contrast of the PEO is larger and positive. This confirms that it is mainly the PEO which is observed in SAXS. The presence of dissolved PEO chains are also supported by the observed q^{-2} behavior at large q in the SANS data. If a model should be constructed from the available information, it should consist of a homogeneous and spherical PPO core and a shell of dissolved PEO chains.

The $p(r)$ functions indicate that the particles have an approximate spherical symmetry and the oscillations in the SAXS scattering curve show that the size polydispersity is small. It is therefore reasonable to apply the square-root deconvolution procedure to the $p(r)$ functions [4,5]. In this procedure the excess scattering length density distribution $\Delta\rho(r)$ is parameterized by a set of step functions. The $p(r)$ is calculated from $\Delta\rho(r)$ and least-squares fitted to the $p(r)$ function from the indirect Fourier transformation. A smoothness constraint is applied and the coefficients in the parameterization are optimized by non-linear least-squares methods. The resulting $\Delta\rho(r)$ functions are shown in Fig. 2(b). The function for the SANS data shows the expected high density core and a lower density shell. The function for the SAXS data also shows the expected behavior with a small negative value in the core and a larger positive value in the shell region. This is in perfect agreement with the calculated contrasts. Note that the size of the core agrees quite well for the two $\Delta\rho(r)$ functions, but that the functions do not go to zero at the same r value. The disagreement at large r is probably explained by the fact that the neutrons are not very sensitive to the low concentration part of the shell with the PEO chains.

The information from the model-independent approaches suggests that the form factor given by Eq. (74), for a particle with spherical core and Gaussian chains attached to the surface, is appropriate to use for fitting the data. The number of fitting parameters in the model is quite large and in order to reduce it, some of the parameters were estimated from other measurements. The excess scattering length densities were calculated from the composition of the P85 triblock copolymer and the specific volumes, which can be derived from density measurements [83]. The contour length of the PEO chains were calculated to be 90 Å using the parameters given by Flory [85] and Aharoni [84].

The inter-particle interference effects are quite small for the low concentrations (0.5–1% wt.), but as the chains extend into the solvent, they are not completely negligible. Therefore, the inter-micellar effects were included in the analysis of the data using a hard-sphere structure

factor (Eq. (83)). As the conditions for the SANS and SAXS measurements are not identical, it was not attempted to fit the two data sets simultaneously. Instead a strategy was chosen, in which only the SANS data were fitted and the results were used for calculating a SAXS scattering curve which was compared to the recorded data.

The theoretical scattering curve was smeared by the instrumental resolution function [23], when the fit to the SANS data was performed. For each setting the appropriate resolution function was used. The fitting was carried out as described in Section 2.2 by combining grid searches with more advanced procedures.

It turns out that the oscillations in the model form factor are too pronounced compared to the experimental scattering curve. Therefore, size polydispersity of the micelles was included using a Schulz distribution for the aggregation number. Note that similar distributions are predicted by thermodynamic equilibrium theories for surfactant micelles [86,87]. In a first attempt the core was assumed to be constituted solely by the PPO parts of the chains. The distance from the surface of the core to the starting points of the Gaussian chains was a fitting parameter.

The polydisperse model fits the scattering data reasonably well. The main deviations are in the region where there is a crossover in the scattering data to the q^{-2} behavior. In order to achieve perfect agreement in this region it was necessary to include a low density PEO shell around the core in accordance with the suggestion by Mortensen and Pedersen [80]. It should be noted that the excluded volume interaction between the chains is not included in the model. As the concentration of chains is quite large at the surface, it is likely that the region closest to the PPO core is more homogeneous than the region further away.

For a model with a PPO core with a low density shell of PEO and dissolved PEO chains, the average aggregation number was $N_{agg} = 74$ which corresponds to a radius of the PPO core of $R = 40$ Å. The additional shell contains 23% of the PEO chains with a water content of 77%. The outer radius of this shell is 49 Å. The Kuhn length is determined to be $b = 10$ Å, which agrees well with previous estimates [84]. The starting point for the PEO chains is $0.25 \times R_g$ away from the surface of the PEO core shell. The polydispersity of the aggregation number is $\sigma(N_{agg})/N_{agg} = 0.37$, where $\sigma(N_{agg})$ is the standard deviation of the Schultz distribution. The corresponding polydispersity of the radius of the core is $\sigma(R)/R \approx 0.13$. This relatively large polydispersity could explain why the shear-induced single crystal BCC phase observed at higher concentration

possesses only angular order and not positional order [88].

The corresponding scattering intensity of the resulting model for X-rays was calculated and is shown in Fig. 1. The model intensity curve reproduces the pronounced oscillation close to $q = 0.1$ Å^{-1} in the measured data and a reasonable qualitative agreement is obtained.

The analysis described in the present section demonstrates the various steps in a typical analysis. The model-independent methods were used for obtaining information on the shape of the micelles and identifying the different components of the structure. A model was constructed from the available information and fitted to the data using least-squares methods. Detailed structural information was obtained on the micellar structure from the analysis.

5. Summary and conclusions

Analysis of small-angle scattering data for colloidal systems consisting of particles or polymers in a solvent has been discussed. Only systems with short range correlations have been considered. Systems with long-range order have sharp Bragg reflections, which can be resolution limited, and the analysis of the data can be quite different from the analysis described in the previous section. In the cases where the system possesses order similar to that of a single crystal, the orientation of the sample also has to be considered. A complete description of the three-dimensional scattering geometry is required and this is quite complicated [89].

A typical data analysis involves both a step with model-independent analysis and a step in which a model on analytical form is fitted to the data. The model-independent step can be an indirect Fourier transformation that involves linear least-squares fitting. In some cases it can be supplemented by a square-root deconvolution which gives the scattering length density profile. The square-root deconvolution requires the application of non-linear methods. A model may be constructed based on the information obtained from the model-independent approaches, but any additional available information on the systems should also be considered. An example of an application of the model-independent approaches and of model fitting was given in the previous section.

The indirect Fourier transformation [1] described in Section 2.1 concerns the three-dimensional distance distribution function, and it is best suited for particles with shapes that are not too anisotropic.

However, a similar approach can be applied for obtaining cross-section distance distribution functions for particles with large anisotropies [2,90]. For infinitely long rods and infinitely large two-dimensional planar structures the scattering from the overall dimension and the cross-section separate. This means the scattering can be written as the product of a power law and a Fourier transform of the cross-section distance distribution function. For rods the power law is q^{-1} and the basis function in the Fourier transform are zeroth order Bessel functions. For planar structures, the power law is q^{-2} and the basis functions are cosines. If the cross-section structure has centro symmetry, it is possible to apply the square-root deconvolution procedure and obtain the cross-section excess scattering length density distribution [4,5]. An example with an application to planar structures has been given by Maurer, Glatter and Hofer [91]. In this study the cross-section structure of large lipid vesicles was determined by SAXS. Applications to rod-like particles have been described by Schurtenberger, Jerke, Cavaco, and Pedersen [92]. The cross-section structure of inverse lecithin micelles with a small core of H_2O and D_2O in deuterated cyclohexane was determined by SANS. The water and lecithin distributions were determined from the difference between the scattering length distribution of the particles with H_2O and D_2O.

The fact that the scattering from the cross-section and the scattering from the large dimension(s) separate for particles with large anisotropies can also be used for extending the available form factors. For planar structure one has, if the cross-section dimension is small compared to the overall size:

$$P(q) = P(q)' P_{cs}(q) \tag{91}$$

where $P(q)'$ is the form factor of an infinitely thin shell describing the overall shape of the object and:

$$P_{cs}(q) = \left| \int \Delta\rho_{cs}(r) \cos(qr)\, dr \right|^2 \tag{92}$$

where $\Delta\rho_{cs}(r)$ is the centro symmetric cross-section scattering length density distribution function. $P(q)'$ can be the form factor of an infinitely thin spherical shell, elliptical shell, cylinder shell, or disk.

For particles with a local rod-like structure, the scattering can also be written using an expression like Eq. (91), if the overall dimension is large compared to the cross-section dimension. In this case

$$P_{cs}(q) = \left| 2\pi \int \Delta\rho_{cs}(r)\, 2B_0(qr) r\, dr \right|^2 \tag{93}$$

where $\Delta\rho_{cs}(r)$ is again the centro symmetric cross-section scattering length density distribution function. $P(q)'$ can be the form factor of an infinitely thin rod (Eq. (66)) or a semi-flexible polymer chain with or without excluded volume interactions [51,93].

The construction of a model cross section may be a tedious job. First the most important features of the structure have to be identified, so that a model structure can be formed. But occasionally, analytical expressions are not available for the scattering cross section of the model structure and it is necessary to construct them or calculate them. This was the case for the P85 micelles described in the previous section. When analytical expressions are derived, it is often convenient to use Monte Carlo simulations [94] for checking the analytical expressions as it was done for the P85 micelles [59]. In some cases it may be impossible to obtain analytical expressions as it is for semi-flexible polymers. If scattering functions are available, for example, from computer simulations for a large range of parameters, the scattering functions can be parameterized and interpolated, so that they can be used for least-squares fitting [51,53,93].

When fitting experimental data, it is not unusual that the information content of a data set is quite low. The parameters of the model are then very correlated and when physical parameters like the mass density are calculated from the fit parameters it may give unphysical values. Such problems can be greatly reduced if the data are on an absolute scale and the molecular properties of the constituting molecules are taken into account in the model as constraints. If the densities are known from other types of measurements this information can be included and unphysical solutions can be avoided. The information content of the data can also be enhanced by measuring for several different contrasts, or by measuring the samples by both X-ray and neutron scattering. For neutrons the contrast variation can be done by varying the deuterated fraction of the solvent. If the particles have components with different composition, the contrast variation will provide additional information. The combination of X-ray and neutron scattering is in some cases very efficient ([95], see also previous section). This is the case for surfactant systems with heavy atoms in the head group, for which the X-ray scattering is almost entirely from the head group region, where as the micelles appear to be homogeneous for

neutron scattering in D_2O. The extra information from contrast variation is most efficiently taken into account if the data from different contrasts are fitted simultaneously. In this case the same parameters for the geometry can be used and only the scattering length densities depend on which contrast is considered.

Acknowledgments

I thank Götz Jerke, Lise Arleth, Kell Mortensen, Michael Gerstenberg and Peter Schurtenberger for their comments on the manuscript.

References

[1] O. Glatter, J. Appl. Cryst., 10 (1977) 415–421.
[2] O. Glatter, J. Appl. Cryst., 13 (1980) 577–584.
[3] O. Glatter, J. Appl. Cryst., 12 (1979) 166–175.
[4] O. Glatter, J. Appl. Cryst., 14 (1981) 101–108.
[5] O. Glatter and B. Hainish, J. Appl. Cryst., 17 (1984) 535–441.
[6] O. Glatter, J. Appl. Cryst., 13 (1980) 7–11.
[7] J.S. Pedersen, J. Appl. Cryst., 27 (1994) 595–608.
[8] H.B. Stuhrmann, Z. Phys. Chem. (Frankfurt), 72 (1970) 177–184, 185–198.
[9] D.I. Svergun, Acta Cryst. A 50 (1994) 391–402.
[10] D.I. Svergun, M.H.J. Koch and I.N. Serdyuk, J. Mol. Biol., 240 (1994) 66–77.
[11] D.I. Svergun, M.H.J. Koch, J.S. Pedersen and I.N. Serdyuk, J. Mol. Biol., 240 (1994) 78–96.
[12] D.I. Svergun, M.H.J Koch, J.S. Pedersen and I.N. Serdyuk, Proc. Natl. Acad. Sci. USA, 91 (1994) 11826–11830.
[13] Data Reduction and Error Analysis for the Physical Sciences. McGraw-Hill, New York, 1969.
[14] W.H. Press, B.P. Flannery, S.A. Teukolsky and W.T. Vetterling, Numerical Recipes. University Press, Cambridge, 1989.
[15] P.B. Moore, J. Appl. Cryst., 13 (1980), 168–175.
[16] D.I. Svergun, A.V. Semenyuk and L.A. Feigin, Acta Cryst., A44 (1988) 244–250.
[17] D.I. Svergun, J. Appl. Cryst., 26 (1993) 258–267.
[18] S. Hansen and J.S. Pedersen, J. Appl. Cryst., 24 (1991) 541–548.
[19] D.I. Svergun and J.S. Pedersen, J. Appl. Cryst., 27 (1994) 241–248.
[20] J.S. Pedersen, S. Hansen and R. Bauer, Eur. Biophys. J., 23 (1994) 379–389.
[21] D.I. Svergun, J. Appl. Cryst., 25 (1992) 495–503.
[22] C.L. Lawson and R.J. Hanson, Solving Least Squares Problems. Prentice-Hall, New Jersey, 1974.
[23] J.S. Pedersen, D. Posselt, and K. Mortensen, J. Appl. Cryst. 23 (1990) 321–333.

[24] D.I. Svergun, J. Appl. Cryst., 24 (1991) 485–492.
[25] D.I. Svergun, Private communication, 1993.
[26] J.S. Pedersen, Implemented in the program GLATTER.FOR, based on the method in Ref. [1].
[27] D.W. Marquardt, J. Soc. Ind. Appl. Math., 11 (1963) 431–441.
[28] B. Sjöberg, J. Appl. Cryst., 11 (1978) 73–79.
[29] J.S. Pedersen, J. Phys. IV France, Coll. C8 3 (1993) 491–498.
[30] J.G. Barker and J.S. Pedersen, J. Appl. Cryst., 28 (1995). 105–114.
[31] J.S. Pedersen, Implemented in the program LSQRES.FOR.
[32] M. Kotlarchyk and S.H. Chen, J. Chem. Phys., 79 (1983) 2461–2469.
[33] Lord Rayleigh, Proc. Roy. Soc. London, Ser. A, 84 (1911) 25–38.
[34] P. Debye, Ann. Phys. Leipzig 46 (1915) 809–823.
[35] A. Guinier, Ann. Phys., 12 (1939) 161–237.
[36] P. Mittelbach and G. Porod, Acta Physica Austriaca 15 (1962) 122–147.
[37] P. Mittelbach and G. Porod, Acta Physica Austriaca 14 (1961) 185–211.
[38] R.W. Hendricks, J. Schelten and W. Schmatz, Phil. Mag., 30 (1974) 819–837.
[39] P.A. Dubey, Dr.sc.nat. Dissertation No. 9077. ETH Zürich, 1990.
[40] P.A. Dubey, B. Schönfeld and G. Kostorz, Acta Metall. Mater., 39 (1991) 1161–1170.
[41] F. Rodríguez, J.C. Gómez Sal, M. Moreno, A. de Geyer and C. Janot, Phys. Rev. B 43 (1991) 7519–7526.
[42] G. Fournet, Bull. Soc. Fr. Minéral. Crist., 74 (1951) 39–113.
[43] P. Mittelbach and G. Porod, Acta Physica Austriaca 14 (1961b) 405–439.
[44] S. Cusack, J. Mol. Biol., 145 (1981) 541–543.
[45] T. Neugebauer, Ann. Phys. (Leipzig), 42 (1943) 509–533.
[46] O. Kratky and G. Porod, J. Colloid Sci., 4 (1949) 35–70.
[47] J. Teixeira, J. Appl. Cryst., 21 (1988) 781–785.
[48] H.D. Bale and P.W. Schmidt, Phys. Rev. Lett., 53 (1984) 596–599.
[49] P. Debye, J. Phys. Colloid Chem., 51 (1947) 18–32.
[50] H. Utiyama, Y. Tsunashima and M. Kurate, J. Chem. Phys., 55 (1971) 3133–3145.
[51] J.S. Pedersen and P. Schurtenberger, Macromolecules (1996) in press.
[52] O. Kratky and G. Porod, Rec. Trav. Chim. Pays-Bas, 68 (1949) 1106–1122.
[53] T. Yoshizaki and H. Yamakawa, Macromolecules, 13 (1980) 1518–1525.
[54] H. Benoit, J. Polym. Sci., 11 (1953) 507–510.
[55] W. Burchard, K. Kajiwara, D. Neger and W.H. Stockmayer, Macromolecules, 17 (1984) 222–230.
[56] J. Polym. Sci. B: Polym. Phys., 30 (1992) 1387–1390.
[57] J.S. Pedersen and M.C. Gerstenberg, unpublished, 1995.
[58] E.F. Casassa and G.C. Berry, J. Polym. Sci. Part A2, 4 (1966) 881–897.
[59] J.S. Pedersen and M.C. Gerstenberg, Macromolecules, 29 (1996) 1363–1365.
[60] B. D'Aguanno and R. Klein, Chem. Soc. Faraday Trans., 87 (1991) 379–390.
[61] F.J. Rogers and D.A. Young, Phys. Rev., A30 (1984) 999–1007.
[62] G. Zerah and J.P. Hansen, J. Chem. Phys., 84 (1986) 2336–2343.
[63] D.J. Kinning and E.L. Thomas, Macromolecules, 17 (1984) 1712–1718.
[64] R.J. Baxter, J. Chem. Phys., 49 (1968) 2770–2774.
[65] C. Regnaut and J.C. Ravey, J. Chem. Phys., 91 (1989) 1211–1221.

[66] S.V.G. Menon, C. Manohar and K. Srinivasa Rao, J. Chem. Phys., 95 (1991) 9186–9190.
[67] J.B. Hayter and J. Penfold, Mol. Phys., 42 (1981) 109–118.
[68] J.-P. Hansen and J.B. Hayter, Mol. Phys., 46 (1982) 651–656.
[69] F.J. Rogers, J. Chem. Phys., 73 (1980) 6172–6178.
[70] A. Vrij, J. Chem. Phys., 71 (1979) 3267–3270.
[71] C. Robertus, W.H. Phillipse, J.G.H. Joosten and Y.K. Levine, J. Chem. Phys., 90 (1989) 4482–4490.
[72] L. Blum and J.S. Hoye, J. Stat. Phys., 19 (1978) 317–324.
[73] L. Blum, J. Stat. Phys., 22 (1980) 661–672.
[74] H. Ruiz-Estrada, M. Medina-Noyola and G. Nängele, Physica A, 168 (1990) 919–941.
[75] B. D'Aguanno and R. Klein, Phys. Rev., A 46 (1992) 7652–7656.
[76] S.F. Edwards, Proc. Soc. London, 88 (1966) 265–280.
[77] T. Shimada, M. Doi and K. Okano, J. Chem. Phys., 88 (1988) 2815–2821.
[78] H. Benoit and M. Benmouna, Polymer, 25 (1984) 1059–1067.
[79] A. Takanishi and T. Ohta, J. Phys. A: Math. Gen., 18 (1985) 127–139.
[80] K. Mortensen and J.S. Pedersen, Macromolecules, 26 (1993) 805–812.
[81] O. Glatter, G. Scherf, K. Schillén, and W. Brown, Macromolecules, 27 (1995) 6046–6054.
[82] J.S. Pedersen. In: H. Brumberger (Ed.), Modern Aspects of Small-Angle Scattering. Kluwer, 1995, pp. 57–91.
[83] J.K. Armstrong, J. Parsonage, B. Chowdhry, S. Leharne, K. Löhner and P. Laggner J. Phys. Chem., 97 (1993) 3904–3909.
[84] S.M. Aharoni, Macromolecules, 16 (1983) 1722–1728.
[85] P.J. Flory. Statistical Mechanics of Chain Molecules. Wiley, New York, 1969.
[86] P.J. Missel, N.A. Mazer, G.B. Benedek, C.Y. Young and M.C. Carey, J. Phys. Chem., 84 (1980) 1044–1057.
[87] M.M. Stecker and G.B. Benedek, J. Phys. Chem., 88 (1984) 6519–6544.
[88] K. Mortensen, W. Brown and B. Nordén, Phys. Rev. Lett., 68 (1992) 2340–2343.
[89] P. Harris, B. Lebech and J.S. Pedersen, J. Appl. Cryst., 28 (1995) 209–222.
[90] J.S. Pedersen and P. Schurtenberger, J. Appl. Cryst. (1996) In press.
[91] N. Maurer, O. Glatter and M. Hofer, J. Appl. Cryst., 24 (1991) 832–835.
[92] P. Schurtenberger, G. Jerke, C. Cavaco and J.S. Pedersen, Langmuir 12 (1996) 2433–2440.
[93] G. Jerke, P. Schurtenberger and J.S. Pedersen, in preparation.
[94] S. Hansen, J. Appl. Cryst. 23 (1990) 344–346.
[95] L. Arleth, D. Posselt, D. Gazeau, C. Lampent, T. Zemb, K. Mortensen and J.S. Pedersen, Langmuir (1996) submitted.